ICPA
17th INTERNATIONAL CONFERENCE ON PRECISION AGRICULTURE
ConBAP 2026
CONGRESSO BRASILEIRO DE AGRICULTURA DE PRECISÃO E DIGITAL
13-16 July 2026 | Porto Alegre, Brazil
ISPA
AsBraAP

Manifold-Based Time-Lag Analysis of Soil Water Availability and Satellite Vegetation Indices for Irrigation Monitoring in Coffee Plantations

Farangis Johari[1], Ednaldo Ferreira[2], Ronaldo C. Prati[1]

[1] Federal University of ABC (UFABC), Santo André, Brazil

[2] Brazilian Agricultural Research Corporation (Embrapa), São Carlos, Brazil

A paper from the Proceedings of the

17th International Conference on Precision Agriculture and 11th Brazilian Congress on Precision and Digital Agriculture

13-15 July 2026

Porto Alegre, Brazil

Abstract.

Monitoring soil-water availability is essential for irrigation management in perennial crops such as coffee, but dense in situ sensing remains costly and difficult to maintain over large agricultural areas. Satellite-derived vegetation indices, including the Normalized Difference Moisture Index (NDMI) and the Enhanced Vegetation Index (EVI), provide scalable information on canopy conditions. However, accurately characterizing the relationship between vegetation dynamics and soil water availability remains challenging because plant responses are often delayed and nonlinear. Moreover, rainfall events, irrigation schedules, and the temporal resolution of satellite observations can obscure the identification of vegetation response lags. This study proposes and evaluates a geometry-aware framework for lag estimation based on the Riemannian comparison of delay-embedded covariance descriptors. The method extends a previously proposed event-filtered Pearson–Spearman correlation approach by representing local temporal dynamics through covariance and rank-covariance structures on the manifold of symmetric positive definite (SPD) matrices. Filtered soil-water tension and vegetation-index series are transformed into delay embeddings, from which local covariance descriptors are extracted and compared using the Log-Euclidean distance. The framework was evaluated using a plot-level monitoring dataset from a drip-irrigated Coffea arabica field in Brotas, São Paulo, Brazil. For NDMI, both the classical and Riemannian approaches identified a consistent two-day response lag. For EVI, however, the classical baseline identified a weak five-day correlation peak, whereas the Riemannian framework consistently selected a two-day lag. Further analysis revealed situations in which Pearson and Spearman coefficients provided divergent or even opposing indications of the relationship between soil water dynamics and vegetation response, suggesting that their aggregation through a simple arithmetic mean may attenuate the resulting cross-correlation signal and affect lag identification. A sensitivity analysis demonstrated that the Riemannian lag estimates remained stable across the tested embedding dimensions and covariance-window sizes for both NDMI and EVI, indicating that the identified lag was not dependent on a particular parameter configuration. In addition, the geometry-aware framework remained sensitive to similarities in local temporal structure and consistently identified early response patterns. These results demonstrate that covariance- and rank-covariance-based geometric alignment can reveal early temporal response patterns that are not adequately captured by conventional correlation measures, while providing robust lag estimates across different embedding configurations. The proposed framework offers a promising alternative for lag estimation in agricultural time series characterized by delayed,

gradual, or nonlinear vegetation responses.

Keywords.
Riemannian geometry; lag estimation; Symmetric Positive Definite (SPD) Matrices, soil-water tension; vegetation indices; NDMI; EVI; irrigated coffee; precision agriculture, Vegetation Indices (NDMI, EVI), Soil-Water Matric Potential (SMP).

Introduction

In irrigated coffee fields, soil water conditions and canopy spectral responses are not always observed at the same time. After irrigation or rainfall, soil sensors register a rapid change in water status, while the corresponding response in a satellite vegetation index may appear several days later. This delay has been reported in studies of canopy response to soil water limitation and can be influenced by plant regulation, crop stage, atmospheric demand, and satellite acquisition timing (Damm et al., 2022). If soil measurements and vegetation indices are compared only on the same calendar date, part of the crop response may be missed.

This problem is important for coffee because short term variation in soil water does not always produce an immediate canopy signal. Coffee plants can regulate water loss through physiological mechanisms, and the spectral response of the canopy may therefore be delayed or smoothed over time (DaMatta & Ramalho, 2006; Carr, 2001). Field sensors provide frequent measurements of soil water status, but their spatial coverage is limited when large areas must be monitored continuously. Satellite-derived indices can complement field measurements by providing repeated spatial observations of canopy conditions. In this study, we focus on the Normalized Difference Moisture Index (NDMI) as an indicator directly associated with vegetation water content and on the Enhanced Vegetation Index (EVI) as an indirect proxy for canopy water status and vegetation development, both derived from optical remote sensing data (Gao, 1996; Huete et al., 2002).

Several studies have reported that vegetation responses to water availability may occur with a delay rather than immediately. These lags vary with crop type, climate forcing, vegetation structure, and temporal resolution of the data. Previous work has shown delayed vegetation responses to precipitation, drought, and crop water deficit indicators across different agricultural and environmental settings (Kong et al., 2020; Damm et al., 2022; Wang, Zhang, et al., 2025). These studies indicate that lag estimation should be treated as a data dependent step, especially when ground based soil measurements and satellite observations are combined for irrigation monitoring.

A recent study on irrigated coffee explored the temporal relationship between soil water availability and vegetation response using soil water matric potential measurements from porous matrix sensors and Sentinel-2 vegetation indices (Ferreira et al., 2025). The proposed approach combined event filtering, monotonic interpolation, and Pearson–Spearman cross-correlation analysis to estimate vegetation response lags. Using the same field dataset, the study reported a two-day response lag for NDMI, while EVI showed a weaker Pearson–Spearman response with its best lag at five days (Ferreira et al., 2025). This event-based method, which filters irrigation events, provides an interpretable baseline; however, it compares the two-time series primarily through pointwise correlations computed within fixed temporal windows.

Pointwise correlation is useful, but it may not fully describe the local temporal behavior of agricultural signals. Pearson correlation measures the strength of a linear relationship between two variables, whereas Spearman correlation assesses the strength of their monotonic association based on rank ordering. Neither measure directly represents how the signal changes within a short time window. This matters because irrigation events, rainfall, missing satellite observations, interpolation, and serial dependence can all affect the local shape of the soil water and vegetation index series. Consequently, two signals may show weak linear and rank-based associations, as measured by Pearson and Spearman correlations, while still exhibiting strong similarities in shape, temporal dynamics, and overall structure.

To address this limitation, this study proposes a Riemannian lag estimation method based on covariance and rank-covariance descriptors. The filtered soil water and vegetation index series are first converted into delay embeddings. Local covariance matrices are then computed over short windows and compared using the Log-Euclidean distance on the space of symmetric positive definite matrices (Pennec et al., 2006; Arsigny et al., 2007). The estimated lag corresponds to the temporal shift that minimizes the cumulative geometric distance between the local structures of the two embedded series.

The main contributions of this study are as follows:

- A geometry-aware lag-estimation framework is developed for time series from sensor signals of irrigated coffee by combining event-based filtering, delay embedding, and Riemannian comparison of SPD covariance descriptors.
- The lag-estimation problem is formulated as the alignment of delay-embedded covariance trajectories using the Log-Euclidean distance on the SPD manifold. Rather than relying on pointwise Pearson–Spearman correlations, the proposed approach identifies lags by matching local covariance structures, thereby recasting lag estimation as a structural pattern-alignment problem.
- The proposed Riemannian estimator is compared with the event-filtered Pearson–Spearman baseline for NDMI and EVI, and its stability is examined under different embedding dimensions and covariance-window sizes.

2. Materials and Methods

The proposed workflow processes soil-water tension, Sentinel-2 vegetation indices, and auxiliary data through event-based filtering, evaluating them using both the classical Pearson–Spearman baseline and the Riemannian lag-estimation method.

2.1 Agricultural Dataset and Preprocessing

The analysis used the same irrigated coffee dataset as the baseline lag estimation study by Ferreira et al. (2025). The field experiment was conducted in a drip-irrigated Coffea arabica area in Brotas, São Paulo, Brazil. This study focused on plot #4, a 0.62 ha plot monitored with the IrrigaDigital® system and the IGstat porous-matrix sensor developed by Embrapa and Tecnicer Tecnologia. Working with the same plot made it possible to compare the Pearson–Spearman lag estimator with the proposed Riemannian method under identical field conditions. The monitoring campaign covered the period from April 20 to November 17, 2022. For the lag analysis, we used the interval from August 12 to November 17, 2022, when drought episodes and irrigation events were more frequent and the dry-to-wet soil-water transitions were easier to identify.

Soil-water matric potential was monitored using the IGstat system, which incorporates a porous-matrix pneumatic sensor designed to estimate soil-water potential for irrigation management (Vaz et al., 2022). Measurements were recorded several times per day and averaged by date to obtain daily soil-water matric potential values. Rainfall data for Brotas were obtained from CIIAGRO, the Agrometeorological and Hydrological Information System of the State of São Paulo (CIIAGRO, 2024).

Vegetation indices were extracted from Sentinel-2 images covering the same monitoring period. NDMI and EVI were calculated as average values for plot #4 at 10 m spatial resolution. The effective temporal resolution was limited by the Sentinel-2 revisit cycle, which is approximately five days, and by the removal of cloudy or shadowed scenes. Image retrieval, cloud and shadow removal, and plot-level index extraction were performed in QGIS using the RAVI plugin (Arantes, 2025). Missing values in the daily vegetation-index series were reconstructed using Piecewise Cubic Hermite Interpolating Polynomial interpolation (PCHIP) for preserving local monotonic behavior and reduces artificial oscillations between observed satellite dates (Fritsch & Carlson, 1980). The analysis used the fused daily series available in the dataset, obtained by averaging the PCHIP-reconstructed values with the corresponding values predicted by the auxiliary model.

Before lag estimation, the sign of the soil-water tension series was adjusted so that dry-to-wet transitions followed the orientation required by the filtering step. Only nonnegative lags were tested. Event filtering was applied before both lag estimation methods to reduce the influence of inactive periods. The filter used a sliding window of five-day measurement window. Segments were retained when the dry-to-wet change exceeded 1.5 kPa for soil-water tension and 0.19 for the vegetation-index signal. Values outside the detected event segments were set to zero. For the rank-based branch, each filtered signal was converted into within-segment ranks inside contiguous nonzero event segments. This step preserved the ordering of values inside each detected event while reducing sensitivity to absolute magnitude.

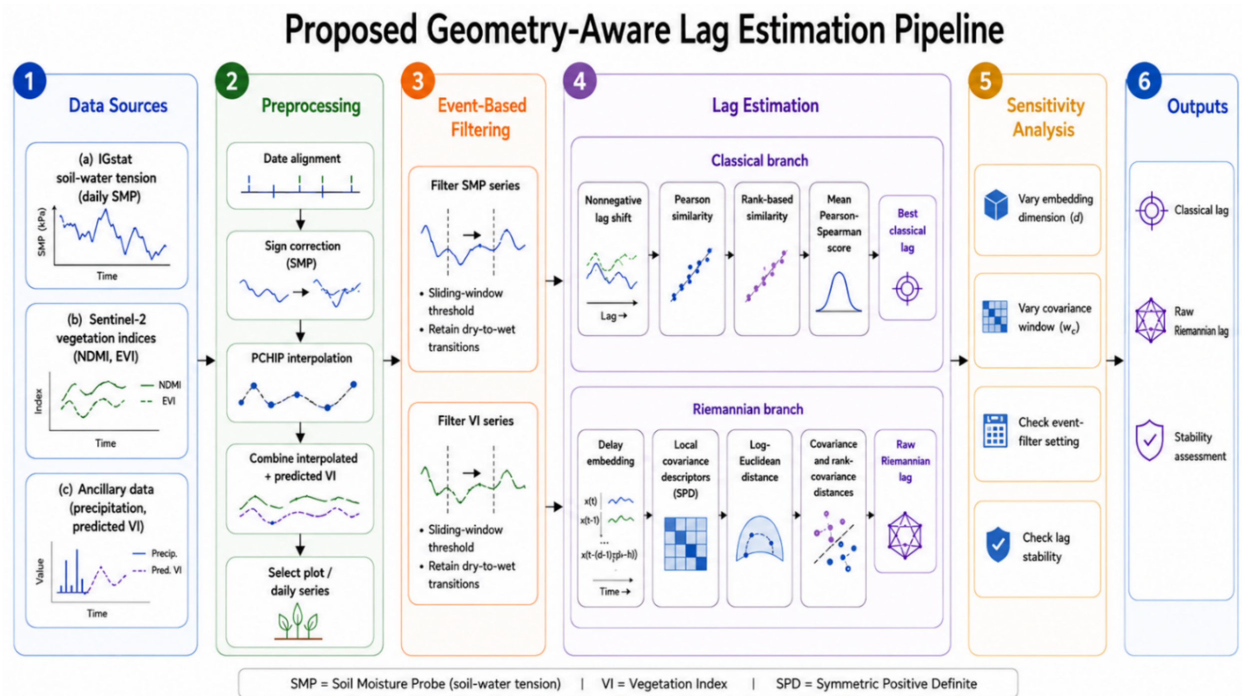

Fig. 1. Proposed geometry-aware lag-estimation pipeline for comparing event-filtered correlation and Riemannian manifold-based lag estimation.

2.2 Cross-Correlation-Based Lag Estimation

The lag-estimation method follows the event-filtered cross-correlation procedure previously applied to the same irrigated coffee dataset by Ferreira et al. (2025). After event-based filtering, the soil-water tension series and the vegetation-index series were compared across a set of candidate nonnegative lags. For each candidate lag, the vegetation-index series was shifted relative to the soil-water tension series, allowing earlier soil-water changes to be compared with later vegetation responses. Following Ferreira et al. (2025), the lag score was calculated as the average of Pearson and Spearman correlation coefficients:

$$r_{PS}(\tau) = \frac{r_{\text{Pearson}}(\tau) + r_{\text{Spearman}}(\tau)}{2}$$

The optimal classical lag was selected as the candidate lag that maximized the Pearson–Spearman score:

$$\tau^{*}_{\text{classic}} = \arg\max_{\tau} r_{PS}\,(\tau)$$

2.3 Geometry-Aware Riemannian Lag Estimation

The Riemannian lag estimator used in this study compares delay-embedded covariance and rank-covariance representations of the signals. After preprocessing and event-based filtering, let $x_f(t)$ denote the filtered soil-water tension series and let $y_f(t)$ denote the filtered vegetation-index series. Here, the generic filtered signal ($s_f(t)$) denotes either the filtered soil-water tension series ($x_f(t)$) or the filtered vegetation-index series ($y_f(t)$), depending on which signal is being delay-embedded.For a generic filtered signal $s_f(t)$, a delay embedding vector is defined as:

$$e_s(t) = \left[s_f(t), s_f(t+1), \dots, s_f(t+d-1)\right]^{\mathrm{T}}$$

where d is the embedding dimension (in our experiments, we set $d = 5$ by default). Local SPD covariance descriptors are then computed from the delay-embedded vectors using a sliding covariance window of length w_c:

$$C_s(t) = \frac{1}{w_c - 1} \sum_{i=0}^{w_c-1} \left(e_s(t+i) - \bar{e_s}(t)\right)\left(e_s(t+i) - \bar{e_s}(t)\right)^{\mathrm{T}} + \varepsilon I$$

Here, $\left(\bar{e_s}(t)\right)$ denotes the mean embedding vector within the covariance window, I is the identity matrix, and $\varepsilon = 10^{-8}$ is a small diagonal regularization parameter that helps keep the covariance descriptors strictly positive definite, $C_s(t) \in S_{++}^d$, especially when a covariance window has low variability. Here, S_{++}^d denotes the space of $d \times d$ symmetric positive definite matrices, meaning that each covariance descriptor is symmetric and has strictly positive eigenvalues.

Because this space is not Euclidean, the proposed method uses the Log-Euclidean distance, which compares SPD matrices through their matrix logarithms while preserving the positive-definite structure of the descriptors (Pennec et al., 2006; Arsigny et al., 2007). For two SPD covariance descriptors A and B, the Log-Euclidean distance is defined as

$$d_{LE}(A, B) = \|\log(A) - \log(B)\|_F.$$

Where $(\log(\cdot))$ is the matrix logarithm computed through eigen-decomposition $(C = U\Lambda U^{\mathrm{T}} \Rightarrow log(C) = U\,log(\Lambda)\,U^{\mathrm{T}})$. For each candidate nonnegative lag $(\tau \in \{0, \dots, \mathrm{K}\})$, where $(\mathrm{K} = 10)$, $\left(\mathrm{C_x(t)}\right)$ is compared with $\left(\mathrm{C_y(t+\tau)}\right)$. Let (V_τ) denote the set of valid aligned covariance-window positions at lag (τ). The covariance-based Riemannian distance is

$$D_{\mathrm{cov}}(\tau) = \sum_{t \in V_\tau} d_{\mathrm{LE}}\left(C_{x_f}(t), C_{y_f}(t+\tau)\right).$$

In parallel, let $x_r(t)$ and $y_r(t)$ denote the rank-transformed soil-water and vegetation-index signals, respectively, with corresponding covariance descriptors are denoted by $C_{x_r}(t)$ and $C_{y_r}(t)$. The rank-based Riemannian distance is computed as

$$D_{\mathrm{rank}}(\tau) = \sum_{t \in V_\tau} d_{\mathrm{LE}}\left(C_{x_r}(t), C_{y_r}(t+\tau)\right).$$

The final Riemannian cost is defined as the average of the covariance-based and rank-based distance curves:

$$D(\tau) = \frac{1}{2}\left(D_{\mathrm{cov}}(\tau) + D_{\mathrm{rank}}(\tau)\right).$$

Therefore, $D(\tau)$ represents the total geometric discrepancy between the aligned local covariance and rank-covariance trajectories local covariance descriptors at a given lag.

The optimal Riemannian lag is then selected as :

$$\tau^* = \arg\min_{0 \le \tau \le \tau_{\max}} D(\tau).$$

3. Results

3.1 Reconstructed Vegetation-Index Time Series

The daily NDMI and EVI series were obtained by combining available Sentinel-2 observations with interpolated values from PCHIP. The NDMI series presents stronger short-term variation and sharper fluctuations than the EVI series, which is consistent with its role as an index more directly related to canopy water condition. The EVI series follows a smoother seasonal trajectory, which is more consistent with its association with canopy greenness and vegetation development. Figures 2(a) and 2(b) show the reconstructed vegetation-index time series used in the lag analysis for plot for NDMI and EVI, respectively.

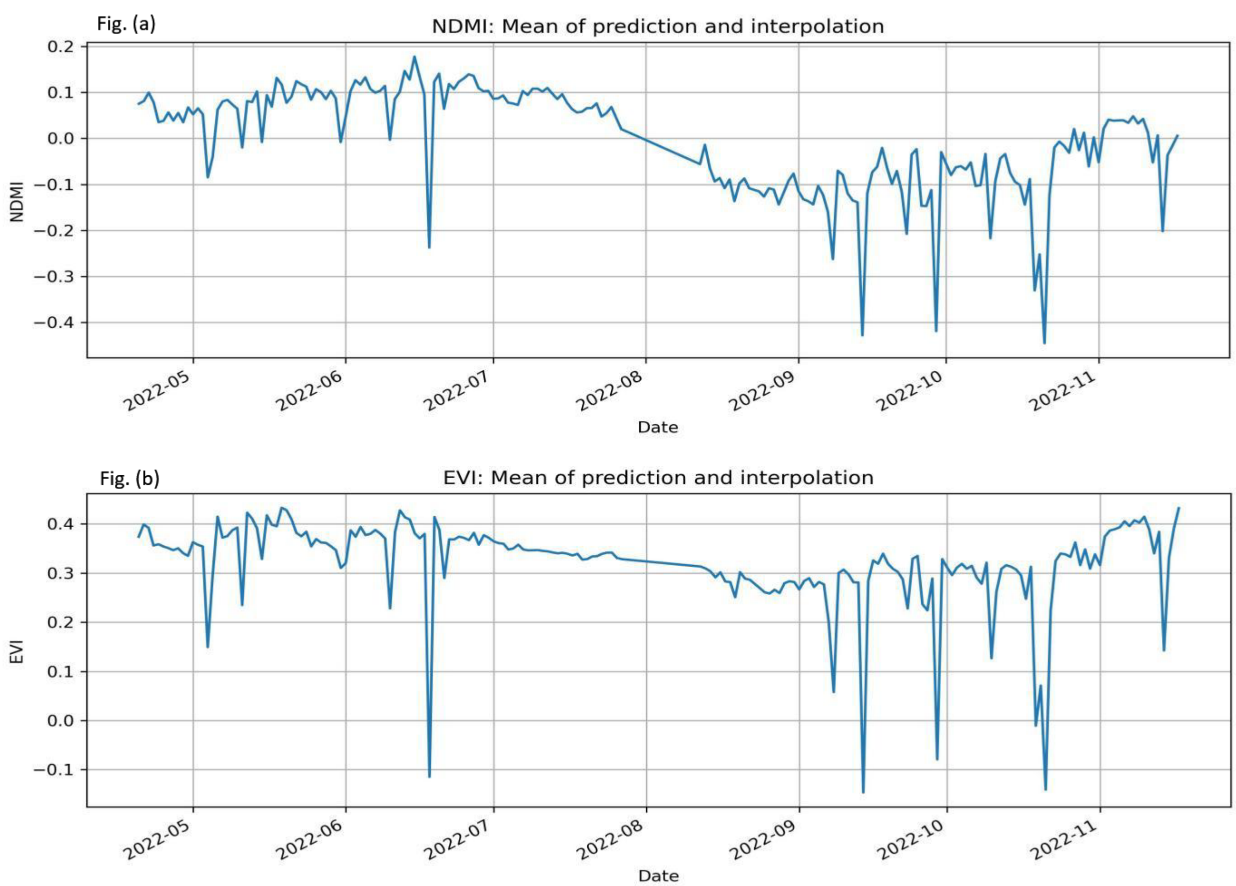

Fig. 2. Reconstructed vegetation-index time series for plot #4: (a) NDMI and (b) EVI. Both series were reconstructed by averaging model-predicted values and PCHIP-interpolated observations.

3.2 Pearson–Spearman Lag Analysis for NDMI and EVI

Table 1 summarizes the best Pearson–Spearman lag obtained for NDMI and EVI. NDMI showed a stronger classical alignment than EVI, with both Pearson and Spearman components supporting a short response delay. For EVI, the average pointwise agreement was weak because the Pearson component was negative, while the Spearman component remained positive. An important implication of the present results concerns the interpretation of the Pearson–Spearman framework adopted by Ferreira et al. (2025). The observed discrepancies between Pearson and Spearman coefficients indicate that linear and monotonic associations do not necessarily provide consistent descriptions of the relationship between soil water dynamics and vegetation responses. In some cases, the two measures even exhibited opposite signs, suggesting fundamentally different interpretations of the same temporal relationship. Under such conditions, combining both coefficients through a simple average may obscure important information and reduce the interpretability of the results. These findings highlight a limitation of pointwise correlation-based approaches for lag estimation. While Pearson and Spearman correlations quantify linear and monotonic associations, respectively, they may not adequately capture similarities in the temporal structure of the signals. In contrast, the proposed manifold-based framework compares local covariance structures in delay-embedded representations, enabling lag estimation through structural alignment rather than pointwise correlation. This characteristic may explain its ability to identify meaningful relationships in cases where conventional correlation measures yield ambiguous or conflicting results.

This pattern suggests that the relationship between soil water dynamics and EVI response may be monotonic but nonlinear, limiting the ability of Pearson correlation to fully characterize the underlying temporal association. Consequently, lag estimates derived from Pearson-based analyses may be biased or suboptimal, as the maximum linear correlation does not necessarily correspond to the true delay governing the vegetation response. This limitation may help explain discrepancies observed in EVI lag estimation and reinforce the need for approaches capable of capturing structural relationships beyond conventional correlation measures.

Table 1. Event-filtered Pearson–Spearman lag estimates for NDMI and EVI in plot #4

Vegetation index	Best lag	Pearson at best lag	Spearman at best lag	Mean
NDMI	2 days	0.611	0.805	0.708
EVI	5 days	-0.504	0.734	0.114

This result highlights an important limitation of averaging Pearson and Spearman coefficients in the Pearson–Spearman baseline. For EVI, the Pearson coefficient was negative while the Spearman coefficient was positive, indicating that the two measures captured different aspects of the soil-water and vegetation-index relationship. Therefore, their simple arithmetic mean may have weakened the resulting lag score and reduced the interpretability of the five-day lag estimate.

3.3 Riemannian Lag-Distance Analysis for NDMI and EVI

Table 2 summarizes the Riemannian results. The Riemannian method selected a two-day lag for both NDMI and EVI. For NDMI, this result agrees with the classical Pearson–Spearman baseline, indicating that the two-day response is expressed through both pointwise association and geometry-aware covariance alignment. For EVI, the Riemannian lag differs from the classical estimate, suggesting that EVI may contain early delay-embedded covariance patterns that are not strongly captured by direct correlation. A possible explanation is that the Pearson–Spearman lag estimate relies on averaging Pearson and Spearman correlations, even when the two measures convey distinct or conflicting information about the temporal association. In such cases, the resulting aggregate metric may mask meaningful structural patterns and lead to suboptimal lag estimates.

Table 2. Riemannian lag distance results for NDMI and EVI in plot #4

Vegetation index	Best lag	Riemannian score
NDMI	2 days	768.936
EVI	2 days	801.779

3.4 Sensitivity Analysis

A sensitivity analysis was performed to examine whether the Riemannian lag estimate changed with the main representation parameters. The embedding dimension was tested at $d \in \{3,5,7\}$, while the covariance window size varied from 3 to 5 daily observations. Table 3 shows that the Riemannian method selected a two-day lag for both NDMI and EVI across all tested parameter combinations. This consistency indicates that the estimated lag was stable and not tied to a single configuration. Notably, variations in the embedding dimension (d) had non-significant effect on the identified lag, suggesting that the proposed framework is robust to the choice of embedding dimension and capable of capturing persistent temporal structures across different representations of the data.

Table 3. Sensitivity analysis of the Riemannian lag estimator for NDMI and EVI under different embedding dimensions and covariance window sizes.

Vegetation index	Embedding dimensions tested	Covariance windows tested	Selected lag across tests	Interpretation
NDMI	3,5,7	3,4,5	2 days	Stable
EVI	3,5,7	3,4,5	2 days	Stable

3.5 Comparison of Pearson–Spearman and Riemannian Lag Estimates

Table 4 directly contrasts the Pearson–Spearman and geometry-aware methods. For NDMI, both approaches identified a two-day lag, indicating that the vegetation response was consistently detectable through both pointwise correlation and delay-embedded covariance structures. This agreement suggests that the NDMI response is sufficiently strong and coherent to be captured by either framework. For EVI, however, the two methods produced different lag estimates. The classical baseline identified a weak correlation peak at five days, whereas the Riemannian method identified a two-day lag. This discrepancy suggests that the EVI response may involve temporal structures that are not adequately represented by conventional correlation measures. As discussed previously, Pearson and Spearman coefficients occasionally provided divergent or even conflicting indications of the underlying relationship, raising questions about the interpretability of lag estimates derived from their combination through a simple arithmetic mean. Under such conditions, the classical estimate may be influenced by the limitations of pointwise correlation analysis, whereas the manifold-based approach remains sensitive to similarities in local covariance structure. Since EVI is more closely related to canopy greenness and vegetation development than to canopy water content alone, its response to irrigation events may be expressed through gradual amplitude changes while still exhibiting early shifts in temporal structure. These early structural adjustments are more readily detected through the analysis of delay-embedded covariance patterns, which may explain the shorter lag identified by the Riemannian framework.

Table 4. Comparison of Pearson-Spearman and Riemannian lag estimates for NDMI and EVI in plot #4

Index	Classical Lag (days)	Pearson-Spearman Score	Riemannian Lag (days)	Min. Distance
NDMI	2	0.708	2	768.936
EVI	5	0.114	2	801.779

4. Conclusion

This study presented a Riemannian framework for estimating temporal lag between soil water tension and satellite-derived vegetation indices in an irrigated coffee field. The proposed method extends the classical event-filtered Pearson–Spearman baseline (Ferreira et al., 2025) by comparing delay-embedded SPD covariance descriptors on a Riemannian manifold, rather than relying solely on pointwise agreement between aligned observations. The framework also incorporates a rank-covariance representation, providing a geometric counterpart to the Spearman component used in the classical baseline.

Using the same plot-level dataset and preprocessing settings as the baseline study, the results showed that NDMI produced a consistent two-day response lag under both the Pearson–Spearman and Riemannian approaches. For EVI, however, the classical baseline identified a weak five-day correlation peak, whereas the Riemannian framework consistently selected a two-day lag. The analysis further revealed situations in which Pearson and Spearman coefficients provided divergent or even opposing indications of the relationship between soil water dynamics and vegetation response. Under such conditions, combining both coefficients through a simple arithmetic means may attenuate or partially cancel the resulting cross-correlation indicator, potentially affecting lag identification. The discrepancy observed for EVI suggests that this effect may have influenced the lag estimate obtained by the classical approach, while the covariance-based geometric framework remained sensitive to early structural changes in the temporal dynamics.

The sensitivity analysis showed that the Riemannian lag estimates remained stable across the tested embedding dimensions and covariance window sizes for both vegetation indices, indicating robustness to parameter selection. Although the study was limited to a single monitored plot, the findings suggest that delay-embedded covariance and rank-covariance representations can complement conventional lag estimation methods in agricultural time series affected by nonlinear vegetation responses, sparse irrigation events, and irregular satellite observations. More broadly, the results indicate that geometric analysis of local temporal structure may provide a useful alternative when correlation-based measures yield ambiguous or conflicting interpretations.

Acknowledgments

This work was funded by the São Paulo Research Foundation (FAPESP) under grants #2025/11944-7 and #2024/15527-9 (SMART project)”. The first author was supported by FAPESP process n°: 2025/25634-0.

References

Arantes, C. (2025). RAVI: Remote analysis of vegetation indices and download of multispectral imagery. QGIS Plugin. https://github.com/caioarantes/ravi-qgis-plugin

Arsigny, V., Fillard, P., Pennec, X., & Ayache, N. (2007). Geometric means in a novel vector space structure on symmetric positive-definite matrices. SIAM Journal on Matrix Analysis and Applications, 29(1), 328–347.

Carr, M. K. V. (2001). The water relations and irrigation requirements of coffee. Experimental Agriculture, 37(1), 1–36.

CIIAGRO - Integrated Center for Agrometeorological Information. (2024). Agrometeorological portal of the state of São Paulo. http://ciiagro.org.br

DaMatta, F. M., & Ramalho, J. D. C. (2006). Impacts of drought and temperature stress on coffee physiology and production: A review. Brazilian Journal of Plant Physiology, 18(1), 55–81.

Damm, A., Cogliati, S., Colombo, R., Fritsche, L., Genangeli, A., Genesio, L., Hanus, J., Peressotti, A., Rademske, P., Rascher, U., Schauemeyer, D., Siegmann, B., Sturm, J., & Miglietta, F. (2022). Response times of remote sensing measured sun-induced chlorophyll fluorescence, surface temperature and vegetation indices to evolving soil water limitation in a crop canopy. Remote Sensing of Environment, 273, 112957.

Ferreira, E., Speranza, E., Vaz, C., Torre Neto, A., Bassoi, L., Rabello, L., Polizeli, J., Bianchi, R., Biondi, G., de Oliveira, F. M. C., Prati, R., & Kamienski, C. (2025). Estimating Vegetation Response Lag to Soil Moisture in Irrigated Coffee Using Porous-Matrix Sensor and Satellite Data. In 2025 IEEE International Workshop on Metrology for Agriculture and Forestry (MetroAgriFor) (pp. 412-417). IEEE.

Fritsch, F. N., & Carlson, R. E. (1980). Monotone piecewise cubic interpolation. SIAM Journal on Numerical Analysis, 17(2), 238–246.

Gao, B. C. (1996). NDWI—A normalized difference water index for remote sensing of vegetation liquid water from space. Remote Sensing of Environment, 58(3), 257–266.

Huete, A., Didan, K., Miura, T., Rodriguez, E. P., Gao, X., & Ferreira, L. G. (2002). Overview of the radiometric and biophysical performance of the MODIS vegetation indices. Remote Sensing of Environment, 83(1–2), 195–213.

Kong, D., Miao, C., Wu, J., Zheng, H., & Wu, S. (2020). Time lag of vegetation growth on the Loess Plateau in response to climate factors: Estimation, distribution, and influence. Science of the Total Environment, 744, 140726.

Pennec, X., Fillard, P., & Ayache, N. (2006). A Riemannian framework for tensor computing. International Journal of Computer Vision, 66, 41–66.

Vaz, C. M. P., Porto, L. F., D'Alkaine, C. V., Bassoi, L. H., Neto, A. T., Hopmans, J. W., & Roiston, D. E. (2022). Design and characterization of a pneumatic micro glass beads matrix sensor for soil water potential threshold control in irrigation management. Irrigation Science, 40(3), 397–405.

Wang, Y., Zhang, Z., Chen, Y., Fan, S., Chen, H., Bai, X., Yang, N., Lin, X., Zhang, Y., & Jin, X. (2025). Correction of crop water deficit indicators based on time-lag effects for improved farmland water status assessment. Agricultural Water Management, 313, 109480.